Problem Chosen	2026 MCM/ICM Summary Sheet	Team Control Number
B		**2618656**

Feeding More, Fairly: Demand-Corrected Scheduling for Mobile Food Pantries

Summary

Keywords: Food Distribution; Truncated Probability; Spatio-Temporal Symbiosis;scheduling

Contents

1 Introduction

1.1 Background

As the paradigm of human space exploration shifts from short-term mission-based landings toward long-term permanent settlement, Earth's finite resources and fragile ecosystems are compelling us to seek extraterrestrial habitats to facilitate the transition toward a multi-planetary civilization. However, traditional chemical-propulsion rockets face inherent bottlenecks, such as low payload ratios, exorbitant launch costs, and irreversible environmental pollution—which struggle to sustain the massive material transport requirements necessary for large-scale Moon Colony construction. Against this backdrop, the Space Elevator System emerges as a revolutionary interplanetary infrastructure [2]. By synergizing with lunar transfer systems, it is designed to establish a green, efficient, and sustainable logistics chain.

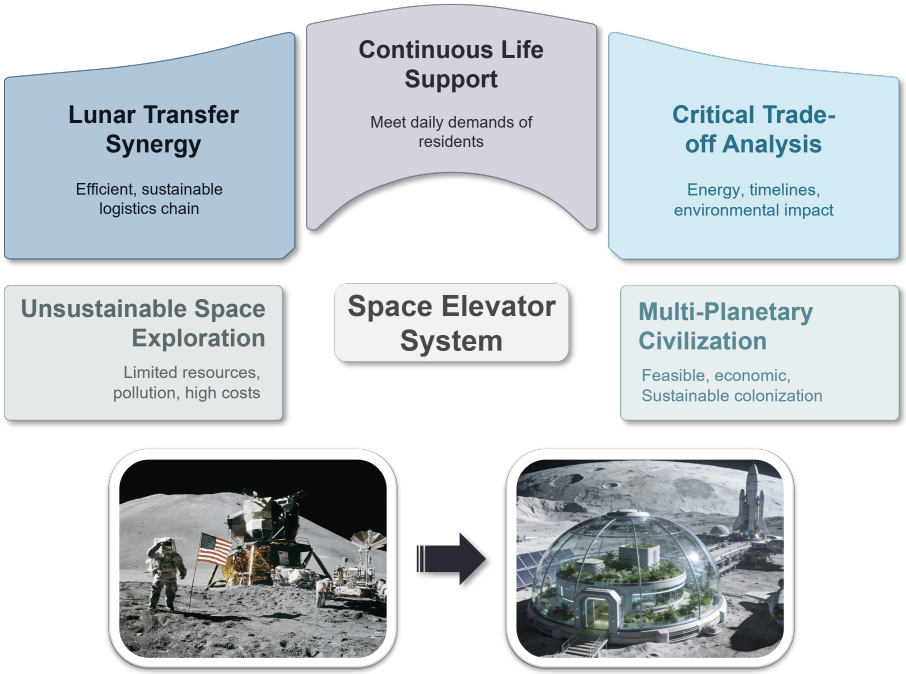

Figure 1: background

The establishment of a large-scale Moon Colony represents both an ultimate test of interplanetary transport capacity and a formidable challenge for the continuous supply of life-support necessities. Within the harsh lunar environment, the daily consumption of 100,000 residents constitutes a persistent logistical demand. When comparing traditional rockets with the emerging Space Elevator System, critical trade-offs must be made regarding energy costs, timelines, launch window constraints, environmental footprints, and the risk-related costs associated with potential system failures. This research is not only central to the feasibility and economic viability of lunar colonization projects but also holds profound significance for the architecture of future interplanetary logistics and the preservation of Earth's ecology.

1.2 Restatement of the Problem

Guided by the constraints provided, we construct a mathematical model to evaluate the optimal cost and schedule for delivering materials to a 100,000-person Moon Colony starting in 2050. The specific tasks are as follows:

- Comparing the logistics and efficiency of three distinct delivery scenarios: utilizing the Space Elevator System's three Galactic Harbours exclusively, relying solely on traditional rocket launches from established sites, or implementing a hybrid transportation strategy .
- Evaluating the robustness of the proposed solutions by analyzing the impact of non-ideal operational conditions, such as mechanical failures or structural instabilities in the elevator and rocket systems .
- Modeling the resource sustainability of the fully operational lunar colony by calculating the additional logistical requirements and costs to ensure a sufficient water supply for one full year .
- Assessing the environmental consequences on Earth's ecosystem under each delivery scenario and optimizing the model to minimize the ecological footprint .
- Providing a strategic recommendation to the Moon Colony Management (MCM) Agency regarding the most viable course of action for building and sustaining the lunar habitat .

1.3 Our Work

2 Model I: Universal Energy-Equivalent and Temporal Coordination Model

2.1 Model Overview

To evaluate Moon Colony logistics, we develop the Universal Energy-Equivalent and Temporal Coordination Model (UETCM). The model adopts Universal Energy-Equivalent (UEE), measured in Joules, as the primary metric to bypass volatile monetary valuations. This thermodynamic baseline facilitates a standardized comparison between the momentum transfer of chemical rockets and the gravitational potential gains of the Space Elevator System.

The modeling process begins with establishing a linear mapping between payload mass and energy consumption, utilizing the Tsiolkovsky rocket equation and gravitational gradients. We then integrate physical constraints, such as site-specific latitudes and launch frequency limits, to optimize logistical efficiency. To resolve the trade-off between timeline and cost, the model employs Pareto front analysis to delineate the decision space for hybrid transport modes, applying the Maximum Distance Method to identify the optimal knee point.

Finally, UETCM is extended into a stochastic model to account for real-world uncertainties. Through 10,000 Monte Carlo simulations, we quantify performance degradation caused by perturbations such as tether swaying, meteorological interference, elevator brake and rocket failures. This approach evaluates the resilience of the Earth-Moon logistics chain, providing a framework that spans from underlying physical mechanisms to strategic decision-making.

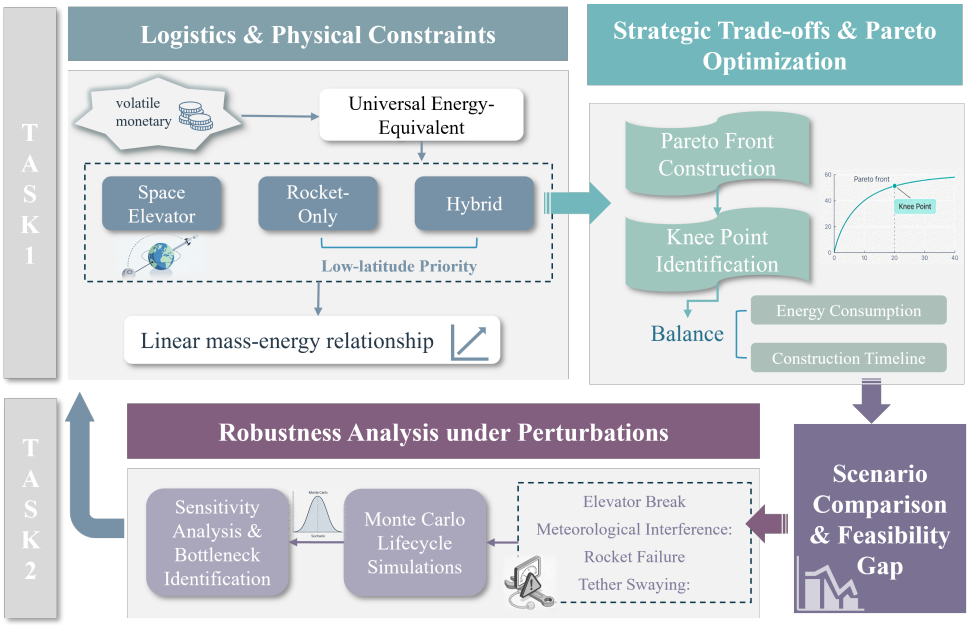

Figure 2: Flow Chart of Model I

2.2 Ideal Energy Cost Modeling

Since the Earth-Moon logistics system spans several decades beyond 2050, this paper discards unstable monetary indicators in favor of Universal Energy-Equivalent (UEE). The selection of this benchmark is guided by several scientific considerations:

- **Economic Invariance:** Monetary values are vulnerable to long-term inflation and geopolitical instability. Utilizing Joules as a measure of energy provides a physical constant across time and space, ensuring the robustness of cost assessments throughout the project lifecycle.
- **Standardized Comparison:** The UEE metric transcends the physical boundaries between chemical propulsion and electrical lift systems. By mapping heterogeneous energy consumption to thermodynamic essentials, it facilitates a fair comparison of energy efficiency across different transport paths.
- **Gravitational Constraint Anchoring:** Interplanetary logistics is essentially the process of overcoming gravitational potential wells. Energy consumption directly quantifies the physical difficulty of breaking gravitational bonds, reflecting potential energy changes and orbital maneuvers more accurately than currency.
- **Resource Sustainability:** In the transition toward a multi-planetary civilization, energy acquisition efficiency and the resource footprint are primary bottlenecks. Using energy as a metric aligns with the requirements of future civilizations for low-entropy and sustainable logistics.

This energy efficiency framework provides a deterministic cost accounting scheme for the post-2050 logistics chain based on the fundamental laws of thermodynamics.

2.2.1 Rocket: Momentum-Based Chemical Propulsion

For traditional rocket schemes, the cost depends primarily on the chemical fuel mass required to lift cargo out of Earth's gravitational potential well. We utilize the Tsiolkovsky rocket equation to explore the relationship between fuel consumption and payload.

Step I: Mass ratio constraint analysis

Consider the velocity increment Δv of a rocket neglecting air resistance. We define the mass ratio R as the ratio of initial mass m_0 to final mass m_f:

$$R = \frac{m_0}{m_f} = e^{\Delta V / v_e}$$

where v_e represents the effective exhaust velocity. For a mission such as Trans-Lunar Injection, ΔV is determined by orbital mechanics and is treated as a constant.

Step II: Linear mapping of fuel consumption to payload

A rocket consists of structural mass such as fuel tanks and engines in addition to the payload. We introduce a structural coefficient α, defined as the ratio of structural mass to fuel mass. Through algebraic derivation, the precise ratio of fuel mass m_{fuel} to payload mass m_p is expressed as:

$$m_{fuel} = \underbrace{\frac{R-1}{1-\alpha(R-1)}}_{k} \cdot m_p$$

This formula distills the flight process into a proportional coefficient k. According to the ideal chemical energy release formula:

$$E_{rocket} = \frac{1}{2} m_{fuel} \cdot v_e^2 = \frac{1}{2} k \cdot v_e^2 \cdot m_p$$

This indicates that under traditional rocket modes, energy cost is a linear function of payload mass.

Step III: Total gravitational potential energy transformation

The total energy consumption ΔE is the sum of overcoming Earth's gravity, lunar gravity compensation, and kinetic energy transitions:

$$\Delta E_{total} = m_p \cdot \left[\left(\frac{GM_E}{R_E} - \frac{GM_E}{d_{EM}} \right) - \frac{GM_M}{2r_M} \right]$$

The terms in the formula represent escaping the Earth's surface, the potential energy difference between Earth and Moon positions, and the energy level transition to enter lunar orbit. Consequently, total energy consumption under rocket transport is linearly proportional to the payload mass.

2.2.2 Space Elevator: Gravitational and Rotational Dynamics

The essential difference between the space elevator and direct rocket flight lies in the primary stage: cargo is first transported along the tether from the Earth Port to the Apex Anchor, then loaded onto a rocket for lunar transit. Since the subsequent rocket segment is covered by the model in the previous section, this section establishes the energy gain model exclusively for the elevator segment.

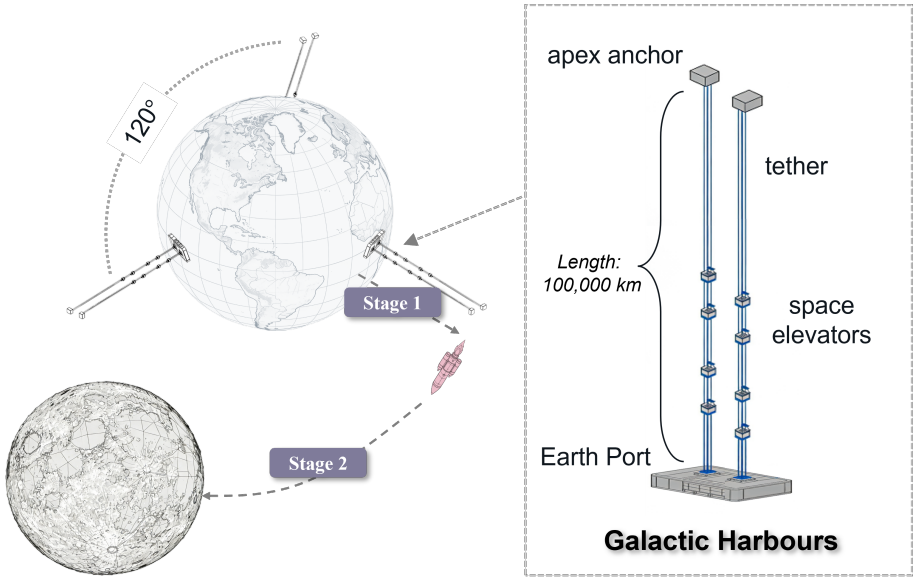

Figure 3: Schematic of the Space Elevator Infrastructure and Earth-Moon Transport Phases

During transport from the Earth Port to the Apex Anchor, the energy change consists of potential energy increase, centripetal kinetic energy gain relative to altitude, and tangential kinetic energy at release:

$$E_{elevator} = m_p \left[\left(\frac{GM_E}{R_E} - \frac{GM_E}{r_0} \right) + \frac{1}{2}\omega^2 r_0^2 \right]$$

where r_0 is the distance from the Apex Anchor to the Earth's center and ω is the Earth's angular velocity. This confirms that elevator transport also maintains a linear relationship between energy consumption and payload.

2.3 Ideal Timeline and Logistic Efficiency Modeling

After resolving the physical energy efficiency, the model determines the construction timeline. The complexity arises from the fact that 100 million metric tons of material cannot be delivered instantaneously; the progress is constrained by the geographical distribution of launch sites, frequency limits, and the inherent capacities of the space elevator and rocket systems.

2.3.1 Transport Progress Formulas

To quantify the construction timeline, the model defines $M_{total} = 10^8$ metric tons as the total demand. Based on the three scenarios provided, the completion time t depends on the annual cumulative capacity C:

- Space elevator only (Scenario a): $t_a = \frac{M_{total}}{C_e}$
- Rockets only (Scenario b): $t_b = \frac{M_{total}}{C_r}$
- Hybrid transport (Scenario c): $t_c = \frac{M_{total}}{\lambda C_e + \mu C_r}$

where C_e is the annual throughput of the space elevator system and C_r is the integrated annual capacity of the rocket system. Shortening the timeline requires increasing annual capacity. By adjusting the hybrid weights λ and μ, we seek a dynamic balance between construction speed and energy cost.

2.3.2 Logistic Efficiency Optimization Under Physio-Geographical Constraints

The primary obstacles to construction progress are geographical constraints and frequency limits, which define the upper bound of C_r.

- **Frequency constraints:** Based on records of ten existing launch sites, we estimate that under ideal conditions after 2050, each site can support at most one launch per day. This ceiling on total annual launch windows determines the minimum possible construction duration.
- **Latitude-based efficiency correction:** Earth's rotation provides rockets with a tangential initial velocity v_{0i}. The energy gain varies by latitude as follows:

$$v_{0i} = v_{0E} \cdot \cos\theta_i$$

As illustrated in Figure 4, higher latitudes result in lower initial velocities, necessitating more chemical fuel. As latitude increases, the non-linear loss of tangential velocity causes the fuel-to-payload ratio to increase from 31.8 at equatorial sites to 34.0 at high-latitude sites.

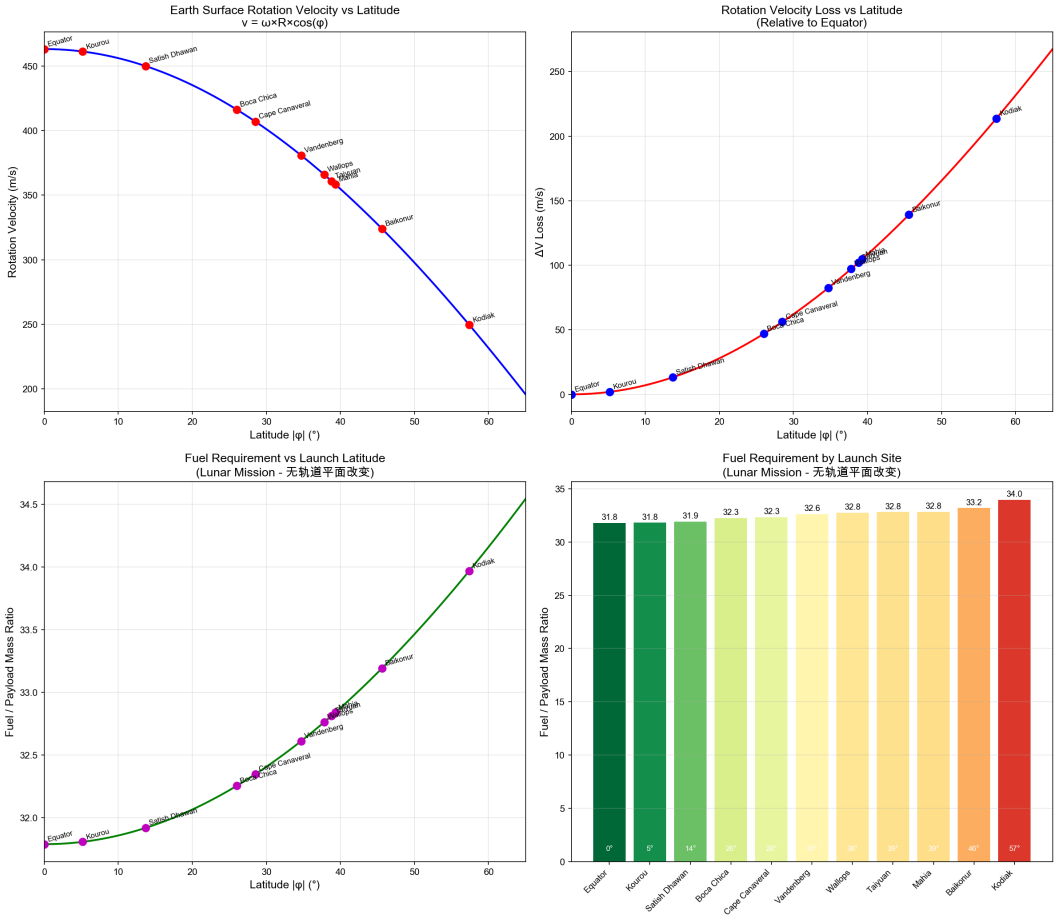

Figure 4: Rotation Velocity and Loss vs Latitude

Consequently, the model implements a low-latitude priority principle: low-latitude sites such as Kourou are prioritized to minimize global energy consumption when the number of launches has not reached the limit. This ensures that for a given timeline, the efficiency of material delivery is maximized.

2.4 Strategic Trade-offs and Multi-criteria Optimization

With the relationship between timeline and cost established, the challenge shifts to strategic decision-making. Since hybrid scenarios must balance energy economy with construction timeliness, we abstract this as a multi-objective optimization problem. Using a Pareto front, we quantify the trade-offs to support the selection of optimal capacity ratios.

2.4.1 Pareto Front and Dynamic Structural Evolution of the Hybrid Scenario

The hybrid transport scenario proposed in the problem is not a static fixed ratio in engineering practice; rather, it represents a continuous spectrum that adjusts dynamically based on the construction timeline objective. By constructing a Pareto front, this model quantitatively defines the internal logical structure of Scenario c.

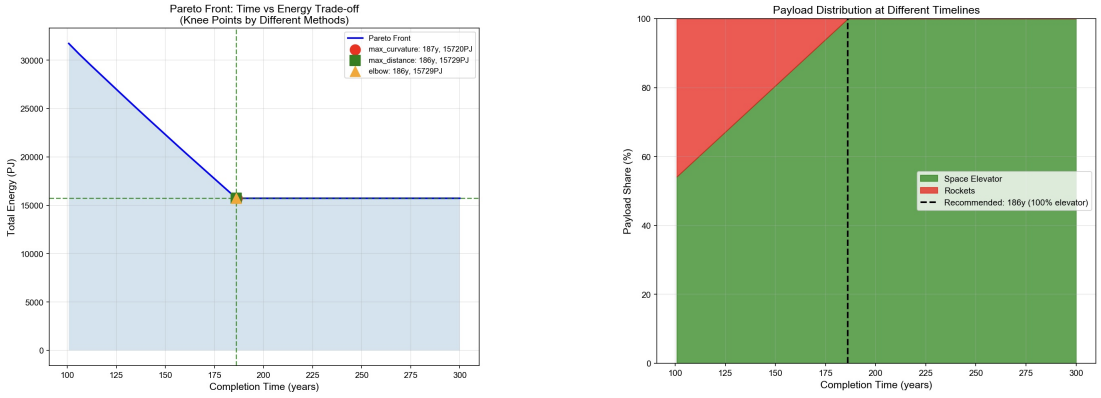

(a) (b)

Figure 5: Energy-Time Trade-off and Payload Distribution in Scenario c

- **Conflict and Trade-off:** As illustrated in Figure 5a, the Pareto front clearly delineates the non-linear negative correlation between energy consumption and the construction cycle. As the planned duration is forcibly compressed, the system is necessitated to increase the proportion of high-energy rocket transport to offset the physical capacity bottlenecks of the space elevator, causing the total energy consumption to surge linearly from the 15,720 PJ baseline.
- **Structural Evolution:** Figure 5b reveals the flexible configuration advantages of the hybrid scheme. When the construction objective is compressed from the ideal 186-year elevator timeline to the 100.7-year hybrid limit, the rocket payload share, indicated by the red region, must be precisely scaled from 0 percent to approximately 45 percent. This logic of automatically deriving the transport structure based on temporal objectives demonstrates the depth and flexibility of the UETCM model in handling complex strategic decision-making.

2.4.2 Knee Point Identification and Marginal Benefit

To avoid arbitrary extremes, the model employs the Maximum Distance to Baseline method to identify the optimal engineering balance point within the Pareto set.

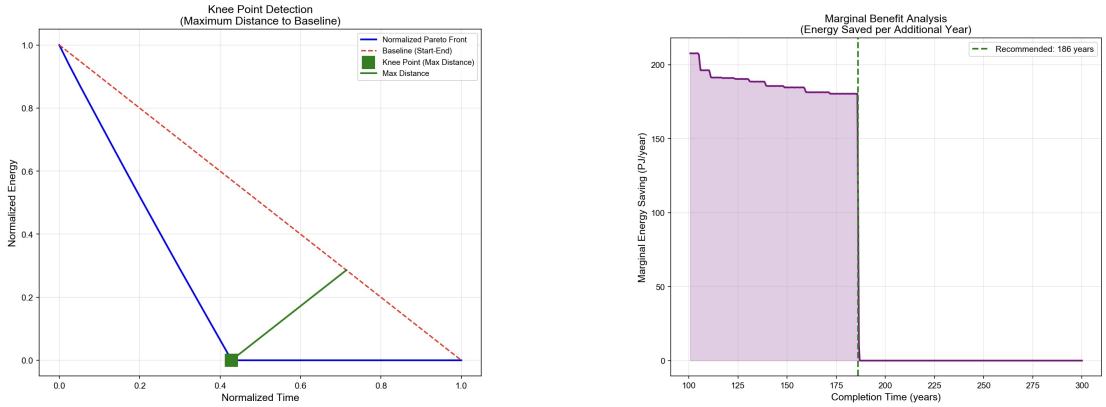

(a) (b)

Figure 6: Knee Point Detection and Corresponding Marginal Benefit Analysis

- Key Point Identification: Figure 6a identifies 186 years as the Cost-Optimal Boundary and 139 years as the multi-objective Knee Point through normalized analysis of energy and duration variables.
- Marginal Benefit Analysis: Figure 6b illustrates diminishing marginal efficiency. Prior to the 186-year boundary, extending the timeline saves an average of 180–210 PJ per year via capacity substitution, reflecting high efficiency in trading time for energy. Beyond this threshold, marginal energy savings drop to zero, establishing the physical limit of optimization.

In summary, the feasible duration for hybrid transport lies between 100.7 and 186.2 years. The upper bound represents the Cost-Optimal Boundary defined by full-load elevator capacity, while the lower bound represents the absolute minimum duration achieved through maximum combined system throughput. Together, these benchmarks demarcate the effective range of the Pareto front.

2.5 Results of Task 1

Through numerical simulation of the 100 million metric ton material transport mission, this study elucidates the intrinsic correlation between construction progress and resource consumption under diverse technical constraints. The findings demonstrate that the optimal transport strategy is not a simple superposition of individual methods but a dynamic equilibrium based on the trade-off between physical energy efficiency and temporal costs.

2.5.1 Quantitative Comparison of Three Transport Scenarios

Based on the model outputs, Table 1 summarizes the core indicators for the three baseline scenarios. The analysis reveals that the hybrid scenario is indispensable for bridging the feasibility gap.

Table 1: Multi-indicator Comparison of Earth-Moon Material Transport Scenarios

Scenario Type	Min Duration (a)	Total Energy (PJ)	Unit Energy (GJ/t)
Space Elevator (a)	186.2	15,720	157.2
Rocket-Only (b)	219.2	50,609	506.1
Hybrid (c)	100.7	31,537	315.4

The detailed analysis is as follows:

1. **Feasibility Gap Analysis**: As illustrated in Figure 7, within the time interval ranging from 100.7 to 186.2 years, the standalone space elevator approach fails to meet objectives due to capacity deficits, while the rocket-only strategy remains unfeasible because of launch frequency limitations. The hybrid scenario represents the sole viable engineering solution within this temporal window.

2. **Efficiency Divide**: Total energy consumption for the rocket-exclusive scenario is 3.2 times that of the space elevator. This energy penalty primarily stems from the propellant mass fraction requirement in chemical propulsion—where additional fuel must be carried to propel the propellant itself—whereas the space elevator system achieves a linearized mass-energy relationship via electrical drive.

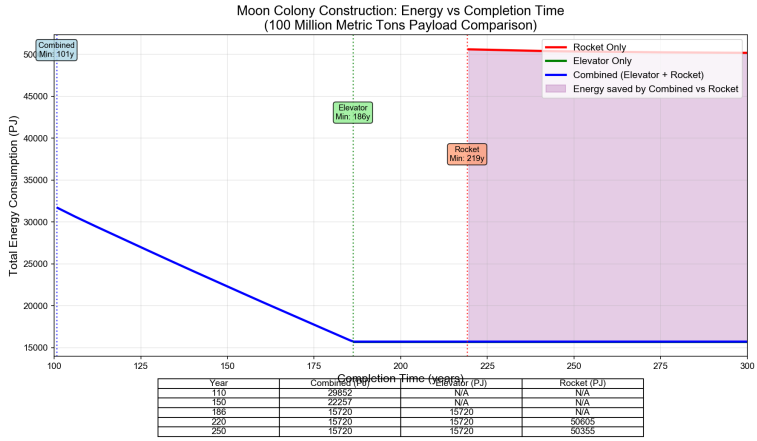

Figure 7: Three Transport Scenarios Feasibility Comparison

2.5.2 Multi-objective Decision-Making via Pareto Front

To optimize the time-energy trade-off, three typical strategies are identified from the Pareto front (100.7–186 years) and detailed in Table 2.

Table 2: Core Metrics of Typical Optimization Strategies for Scenario C

Strategy Type	Duration (a)	Total Energy (PJ)	Elevator Share	Energy Saving
Strategy A (Cost-Prioritized)	186.0	15,720	100.0%	69.0%
Strategy B (Time-Prioritized)	100.7	31,537	54.1%	37.7%
Strategy C (Balanced)	139.0	24,361	74.6%	51.9%

These strategies represent key Pareto nodes: Strategy A minimizes global energy via full-load elevator operation; Strategy B achieves the shortest timeline through maximum energy input; and Strategy C balances construction efficiency with energy expenditure to provide the basis for capacity allocation.

1. **Marginal Energy Saving**: As shown in Figure 8, the marginal saving curve exhibits a step-wise diminishing trend. Between years 101 and 139, each additional year allocated to the timeline reduces energy demand by approximately 210 PJ. Beyond the 139-year knee point, the marginal conservation rate drops to 185 PJ/a, indicating saturation of energy returns for time invested.

2. **Knee Point Recommendation**: The 139-year duration is recommended as the global optimal point. It extends the minimum timeline by only 38 percent while yielding a 22.7 percent reduction in energy consumption. In this configuration, the elevator assumes 74.6 percent of the transport load, achieving an efficient logistical structure.

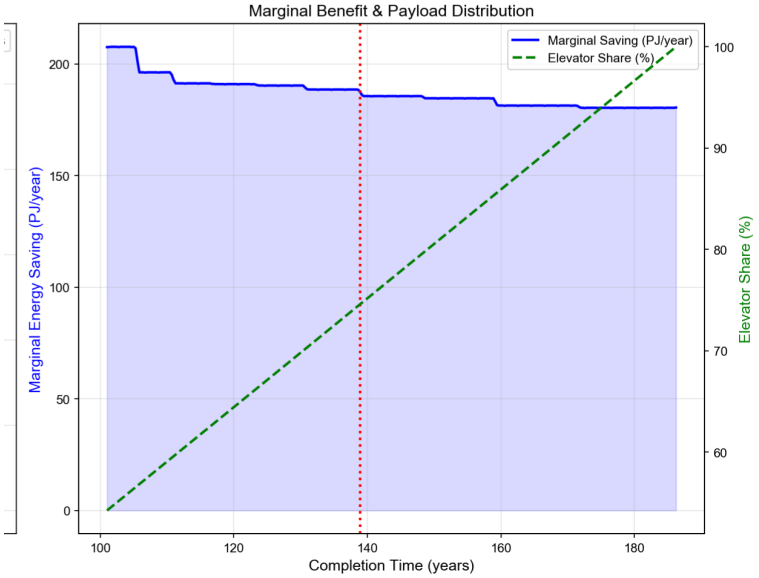

Figure 8: Combined Scenario Pareto Front

2.6 Stochastic Revision Model Under Non-Perfect Working Orders

Idealized models establish a theoretical upper bound for optimization; however, real-world aerospace engineering is fraught with significant uncertainties. To address Task 2, we extend the UETCM into a stochastic model incorporating a perturbation operator δ.

2.6.1 Physical and Logical Quantification of Stochastic Perturbations

Perturbations are quantified across energy efficiency and schedule interruption dimensions, with all factors based on realistic aerospace scenarios:

1. **Mechanical Disturbances**: Oscillations ($\Delta\theta$) of the 100,000 km tether caused by Coriolis forces lead to velocity vector deviations during payload release. This necessitates

additional orbital maneuver energy (ΔE) for correction:

$$\Delta E = \frac{1}{2}(e^{\Delta v_{\Delta\theta}/v_e} - 1)v_e^2 m_p, \quad \Delta v_{\Delta\theta} = \omega r_0 \sin \Delta\theta$$

where $\Delta\theta \sim N(0, 0.5°)$.

2. **Reliability Disturbances**:
   - **Rocket Failure**: Based on historical Falcon 9 logs[1], the baseline failure rate for 2050 is set between 0.5% and 1.0%.
   - **Elevator Break**: Annual failures for the elevator system are set to 2, with downtime following a distribution of $N(14, 16)$ days.
3. **Environmental Disturbances**: A 10% risk of launch site stoppage due to adverse meteorological conditions is incorporated.

2.6.2 Monte Carlo Lifecycle Simulation

Due to the highly non-linear interactions between these stochastic variables, we utilized a Monte Carlo algorithm to execute 10,000 simulations of the construction cycle.

- **Simulation Logic**: For each simulated day, the algorithm samples the system state (Normal/Failure/Weather). In the event of interference, payload distribution is adjusted and incomplete tasks are rescheduled.
- **Distribution Analysis**: As shown in Figure 9, the results exhibit a significant right-skewed distribution. This implies that real-world timelines are prone to a long tail of cumulative delays—the probability of massive delays is low but the impact is profound, serving as a critical basis for risk assessment.

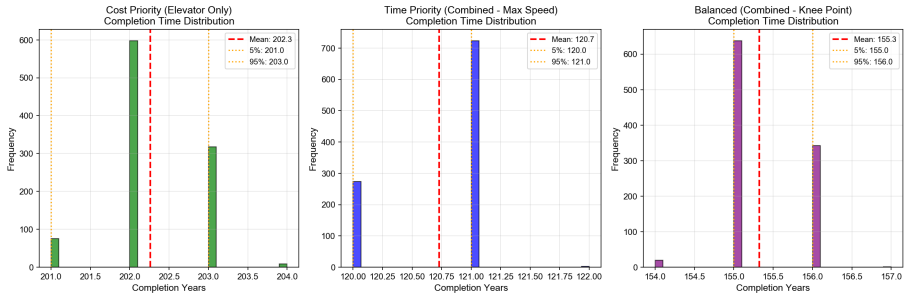

Figure 9: Completion Time Distribution Under Perturbations

2.7 Results of Task 2

Idealized models define the theoretical limits, but stochastic variables such as tether swaying, equipment failure, and weather interference cause performance to deviate. We evaluate system performance under disturbance based on 1,000 Monte Carlo iterations.

2.7.1 Quantitative Comparison of Performance Loss

Table 3 compares the deterministic solutions with stochastic means, quantifying the costs of system perturbations.

Table 3: Comparison of Core Metrics Under Perfect and Non-Perfect Conditions

Strategy Type	Dimension	Perfect Condition	Non-Perfect (Mean $\pm$ Std)	Change Rate
Strategy A	Time (a)	186.2	202.3 ± 0.6	+8.6%
	Energy (PJ)	15,720	$15{,}738 \pm 0$	+0.1%
Strategy B	Time (a)	100.7	120.7 ± 0.4	+19.9%
	Energy (PJ)	31,537	$30{,}217 \pm 30$	-4.2%
Strategy C	Time (a)	139.0	155.3 ± 0.5	+11.7%
	Energy (PJ)	24,361	$24{,}060 \pm 0$	-1.2%

Analysis shows that although Strategy A has the longest absolute duration, its relative delay is minimal and energy consumption remains stable. Its 100% elevator share provides inherent stability, as semi-permanent infrastructure is more resilient than rocket systems. Conversely, Strategy B suffers the highest delay rate due to its heavy reliance on rockets , exposing it to the dual risks of launch failure and weather cancellations. Strategy C maintains its balanced position, validating its role as a robust choice.

2.7.2 Evolution of Key Indicators

Stochastic disturbances transform deterministic values into probability distributions, but the strategic ranking remains robust.

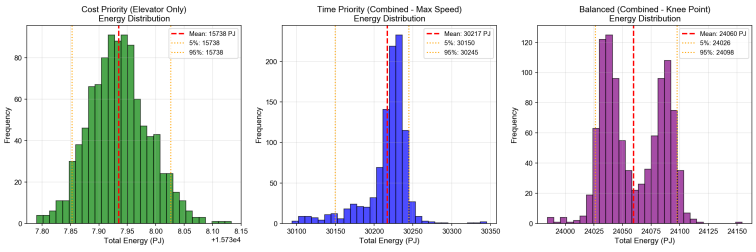

Figure 10: Energy Distribution

- **Energy Stability**: As illustrated in Figure 10, energy consumption follows a narrow-peak normal distribution with a standard deviation of less than 0.2%. This confirms that tether swaying does not cause energy collapse. The slight mean shift in Strategies B and C is due to payload loss from rocket failures offsetting energy increments from swaying.
- **Temporal Right-Skewed Characteristics**: Box plots in Figure 11 reveal that median durations delay by 8.6% to 19.9%. However, the duration intervals for each strategy remain strictly separated, ensuring that the fundamental decision logic—Strategy A for cost and Strategy B for speed—holds true even under perturbation.

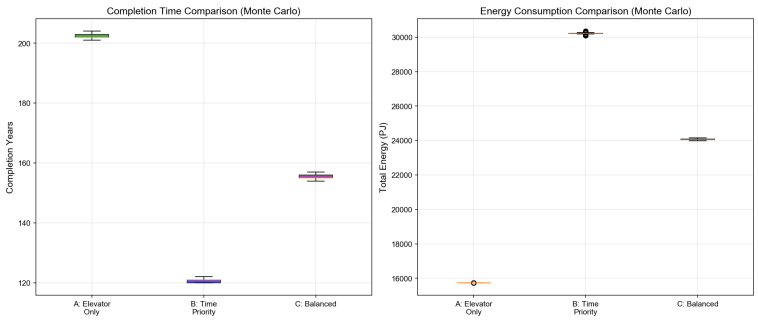

Figure 11: Completion Time and Energy Consumption Comparison

2.7.3 Bottleneck Analysis of Core Perturbation Factors

Attribution and sensitivity analyses (Figure 12 and Figure 13) identify the hierarchy of bottlenecks: **Elevator Break** > **Meteorological Interference** > **Tether Swaying** > **Rocket Failure**.

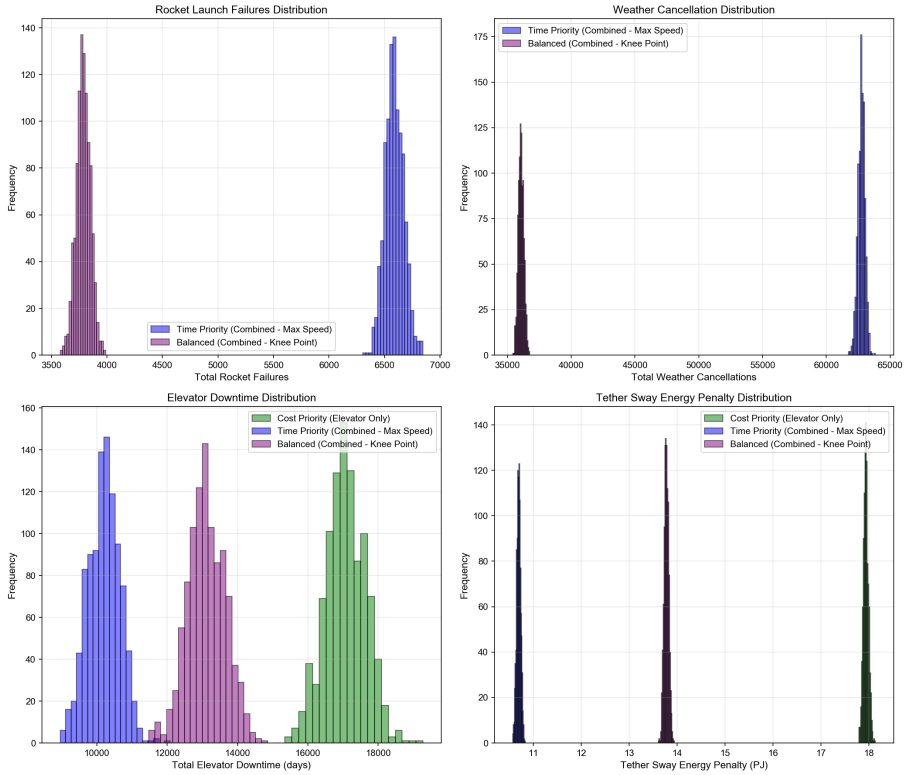

Figure 12: Failure Analysis

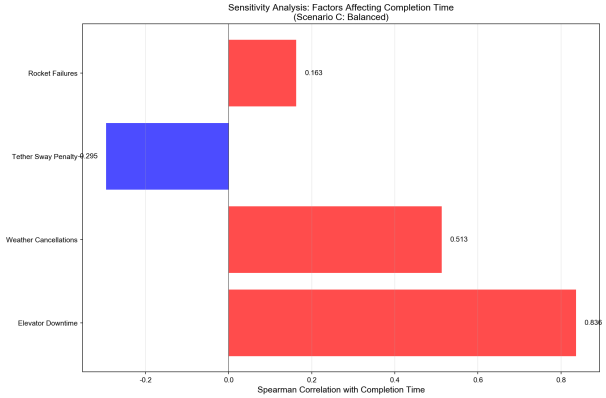

Figure 13: Sensitivity Analysis

- **Elevator Break**: Peak downtime for Strategy A reaches 18,000 days, accounting for 23% of the construction cycle. With a correlation coefficient of 0.836, it is the sole strong correlation factor. As the logistical backbone, any minor fluctuation in elevator availability triggers linear drifts in the timeline.
- **Meteorological Interference**: Weather-induced cancellations occur 9.5 times more frequently than rocket failures. This indicates that site geography and weather, rather than technical reliability, are the primary constraints on rocket efficiency.
- **Rocket Failure and Tether Swaying**: These factors exhibit low correlation (0.163 and -0.295, respectively). Within an engineering control range of $\pm 0.5°$, tether swaying impact is negligible.

3 Life-Support Logistics and Stochastic Water Balance Model

3.1 Model Overview

As the Moon Colony transitions from the construction phase to the operational phase, the logistical focus shifts from structural materials to life-support supplies. We develop the Life-Support Logistics and Stochastic Water Balance Model (LSL-SWBM) to quantify the water security boundaries of the settlement during its first year of operation. This model accounts for multi-level demand functions based on psychological comfort and incorporates a normal approximation to address stochastic medical emergency needs. By mapping these water requirements onto the transport framework established in Model I, we evaluate the additional pressure exerted by different comfort factors on the Earth-Moon logistics chain.

3.2 Water Demand Architecture

In an isolated lunar ecosystem, water consumption is primarily sustained by a recycling system. However, logistical replenishment must compensate for system losses and sudden medical surges. This model assumes that lunar water use is restricted to domestic and medical emergency purposes, excluding industrial use, to define the core demand framework.

3.2.1 Domestic Water Evolution

Within the colony, domestic water consists of survival and hygiene components. The daily demand is formulated as:

$$W_r = N \times (w_s + 0.4\alpha) \tag{1}$$

where N is the population, w_s represents the survival baseline, and α is the comfort factor. The following table summarizes the water standards across different demand tiers:

Table 4: Water Demand Standards Across Different Comfort Tiers

Demand Tier	α **Value**	**Daily Use per Capita**	**Description**
Survival Standard	1	2.9 L	Minimum survival threshold
Comfort Standard	50	22.5 L	Moderate domestic comfort
Luxury Standard	250	102.5 L	Equivalent to Earth-like usage

3.2.2 Stochastic Assessment of Medical Emergency Water

Given the large population , the daily number of patients X (assuming a daily incidence rate $p = 2\%$) follows a binomial distribution, which is accurately approximated by a normal distribution $X \sim N(Np, Np(1-p))$. To ensure medical safety under extreme conditions, the model adopts the peak demand at a 99% confidence level as the daily reserve target:

$$W_{medical} = (E(X) + Z_{0.99} \cdot \sigma) \times 5 \text{ kg} \tag{2}$$

This indicator remains stable across different domestic comfort scenarios, ensuring the robustness of the medical support system.

3.3 Logistics Strategy: Initial Filling and Dynamic Compensation

Unlike construction materials, water is highly recyclable. Given the maturity of water recycling technology, the cumulative rate of daily demand after the initial transport is relatively slow. Since a daily delivery schedule would be prohibitively expensive, we adopt a monthly supply mode based on a dual-stage replenishment logic.

3.3.1 Initial Month Filling

During the first month, recycled water from the previous month is unavailable. Thus, the initial supply must satisfy two criteria: providing domestic water for 30 days and maximizing medical reserves for potential surges. The initial transport volume is defined as:

$$W_{initial} = (W_r + W_{mi}) \cdot T \tag{3}$$

where $T = 30$ days and W_{mi} is the daily emergency medical supply at a 99% confidence level. This strategy establishes the system's circulating base while creating a 30-day emergency buffer.

3.3.2 Monthly Routine Compensation

In subsequent months, domestic demand is met through a combination of Earth-based replenishment and water recycling. Simultaneously, medical reserves need only cover the mean incidence

rate due to the confidence buffer established initially. With a recycling efficiency η (set at 0.9), the routine monthly supply model is:

$$W_{routine} = (W_r(1-\eta) + W_m) \cdot T \tag{4}$$

This model precisely offsets recycling losses and daily medical consumption to maintain a dynamic water balance.

3.4 Results and Multi-dimensional Analysis for Task 3

Based on the model simulation results, we perform a quantitative decomposition of the water replenishment mission across both temporal and energetic dimensions.

3.4.1 Comparison of Demand Scales across Scenarios

Minute variations in the comfort factor α trigger significant shifts in logistical scale. The water demand metrics for the three simulated scenarios are summarized in Table 5.

Table 5: Water Demand Metrics under Different Comfort Scenarios

Demand Tier	α	**Water Inventory** (t)	**Daily Rep.** (t)	**Initial Trans.** (t)	**Annual Total** (t)
Survival Standard	1	290	29.1	1,163	10,622
Comfort Standard	50	2,250	225.1	9,003	82,162
Luxury Standard	250	10,250	1,025.1	41,003	374,162

Table 5 clearly illustrates the multiplier effect of psychological comfort on logistical scale: as the standard shifts from Survival ($\alpha = 1$) to Luxury ($\alpha = 250$), the annual replenishment requirement surges from approximately 10,000 to over 370,000 metric tons— a jump of more than 35-fold.

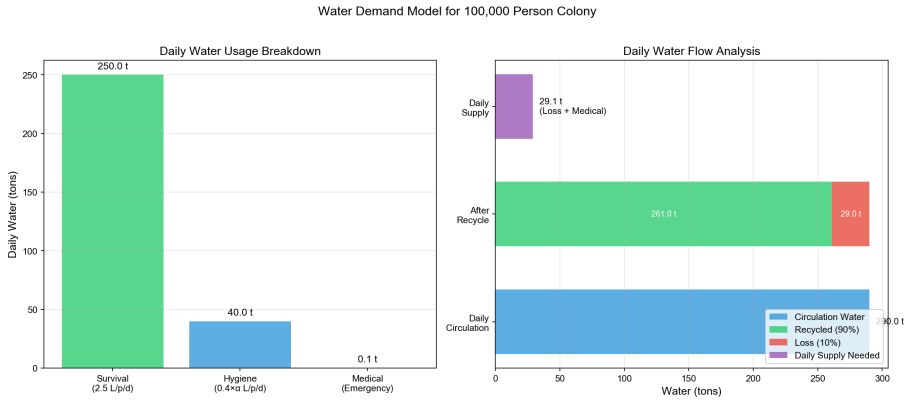

Figure 14: Decomposition of water demand components for the Survival Scenario ($\alpha = 1$)

Taking the Survival Scenario ($\alpha = 1$) as an example, Figure 14 delineates the composition of water demand. Supported by a high-efficiency recycling system, the daily volume required from Earth accounts for only a small fraction of the total demand, underscoring the critical value of closed-loop life-support systems.

3.4.2 Trade-off Analysis of Transport Schemes

To satisfy the aforementioned water requirements, we mapped the demand indicators onto the transport framework of Model I to evaluate four distinct transport schemes. The definitions and baseline capacity comparisons for these schemes are detailed as follows:

Table 6: Definition and Baseline Capacity of the Four Transport Schemes

Scheme	Description	Daily Capacity (t/d)	Specific Energy (GJ/t)
1	Space Elevator Only (3 units)	1,471	157.2
2	Rocket-Only (10 sites)	1,250	506.1
3	Hybrid (Elevator + 10 sites)	2,721	317.5
4	Hybrid (Elevator + Low-lat.)	1,971	243.5

The data indicates that Scheme 3 offers the highest aggregate daily throughput, whereas Scheme 1 provides superior energy efficiency. Although rockets offer viable capacity, their energy cost is approximately 3.2 times that of the space elevator. By integrating the demand tiers with these schemes, we derive the following performance analysis:

(1) Survival Scenario ($\alpha = 1$)

Table 7: Transport Performance Metrics for the $\alpha = 1$ Scenario

Scheme	Initial Days	Initial Energy (TJ)	Monthly Days	Annual Energy (PJ)
Scheme 1	0.79	182.8	0.59	1.67
Scheme 2	0.93	588.6	0.69	5.38
Scheme 3	0.43	369.2	0.32	3.37
Scheme 4	0.59	283.1	0.44	2.59

As shown in Table 7, all schemes can complete monthly replenishment within one day under low-demand conditions. Scheme 1 demonstrates an absolute advantage in efficiency (1.67 PJ/a), while Scheme 3 minimizes delivery time (approx. 10 hours for the initial filling). This suggests that water transport poses minimal pressure on the logistics chain in survival mode.

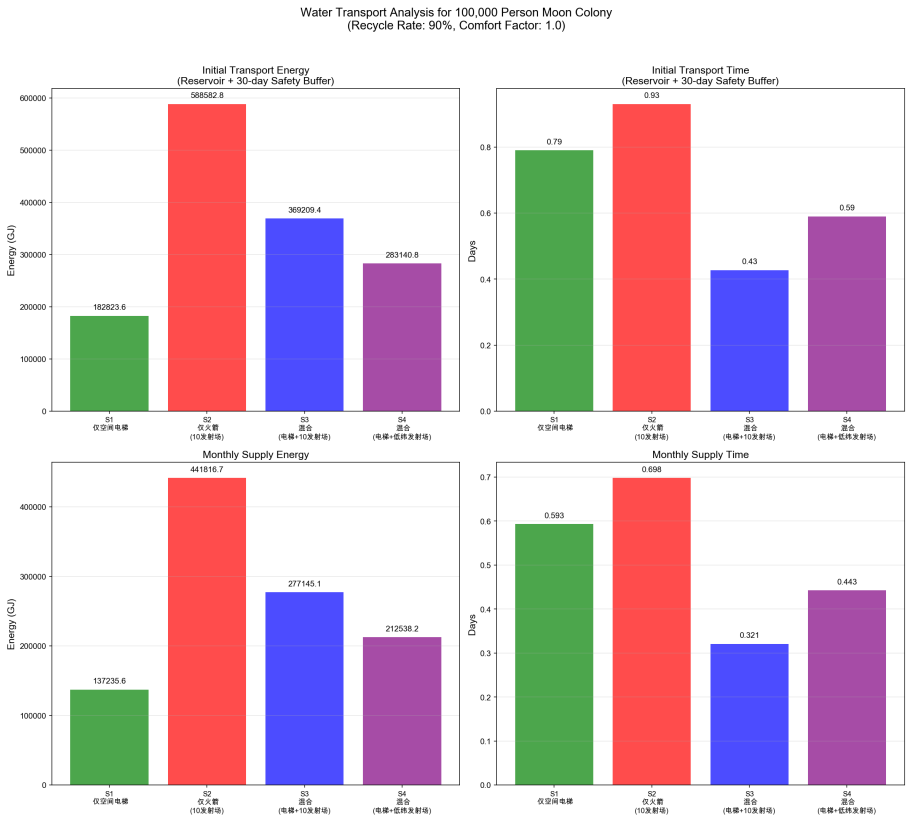

Figure 15: Comparison of transport duration and energy for the $\alpha = 1$ scenario

(2) Comfort Scenario ($\alpha = 50$)

As demand increases eightfold, logistical pressure rises significantly. Under Table **??**, Scheme 1 can still complete initial filling within 6.12 days, though annual energy consumption increases to 12.92 PJ. Scheme 4 provides a well-balanced equilibrium between timeline and energy.

Table 8: Transport Performance Metrics for the $\alpha = 50$ Scenario

Scheme	Initial Days	Initial Energy (TJ)	Monthly Days	Annual Energy (PJ)
Scheme 1	6.12	1,415.3	4.59	12.92
Scheme 2	7.20	4,556.3	5.40	41.58
Scheme 3	3.31	2,858.1	2.48	26.08
Scheme 4	4.57	2,191.9	3.43	20.00

(3) Luxury Scenario ($\alpha = 250$)

In this extreme scenario, water logistics becomes a major logistical burden. Table **??** reveals that relying solely on Scheme 1 requires nearly a month for initial filling, with annual energy consumption reaching 58.82 PJ.

Table 9: Transport Performance Metrics for the $\alpha = 250$ Scenario

Scheme	Initial Days	Initial Energy (TJ)	Monthly Days	Annual Energy (PJ)
Scheme 1	27.87	6,445.7	20.90	58.82
Scheme 2	32.80	20,751.2	24.60	189.36
Scheme 3	15.07	13,016.9	11.30	118.78
Scheme 4	20.80	9,982.5	15.60	91.09

Remarkably, even under the Luxury Standard, the annual energy for water transport (58.82 PJ) accounts for only 0.37% of the total construction energy (15,720 PJ) calculated in Model I. This validates that the primary bottleneck is not energy availability, but rather transport capacity allocation.

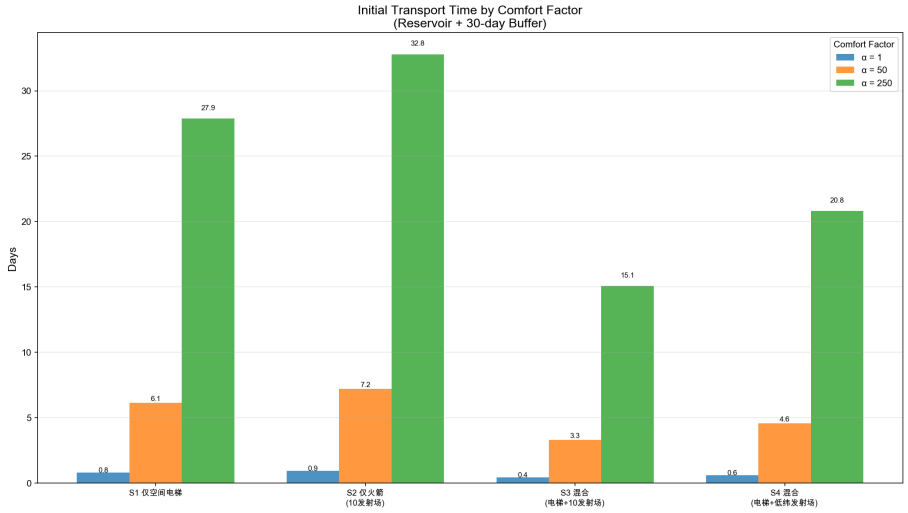

Figure 16: Comparison of initial transport duration across diverse comfort tiers

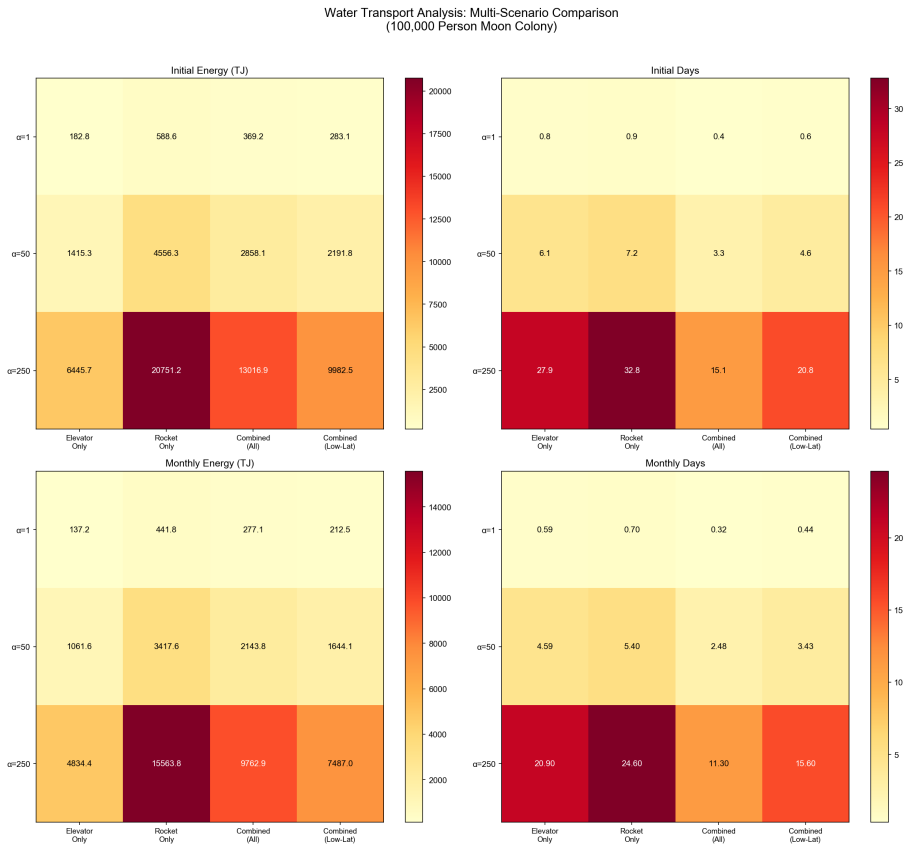

Figure 17: Heatmap of annual energy consumption across scenarios and transport schemes

The heatmap in Figure 17 reveals two critical trends:

1) Energy consumption surges with α for all schemes.

2) For any given α, Scheme 1 consistently exhibits the lowest energy footprint, confirming its superior efficiency.

3.5 Conclusion and Strategic Insights

1. **Trade-off between Comfort and Capacity**: Quantitative analysis confirms that quality of life acts as a logistical amplifier. At the Luxury tier ($\alpha = 250$), the annual water replenishment occupies 69.68% of the theoretical annual capacity of the space elevator system (Scheme 1). Maintaining high living standards significantly constricts the transport window for other critical infrastructure and scientific materials.

2. **Tiered Strategy Recommendations**:

   - **Initial Operations**: We recommend $\alpha = 1$ **(Survival) combined with Scheme 1**. This minimizes energy consumption (1.67 PJ/a) while ensuring the survival threshold for 100,000 residents, reserving hybrid capacity for urgent infrastructure tasks.
   - **Mature Operations**: We recommend $\alpha = 50$ **(Comfort) combined with Scheme 4**. This provides a balance between speed and cost, completing the initial filling in 4.57 days with a reasonable energy footprint.

3. **System Resilience**: Thanks to the 90% efficient recycling system and the 30-day emergency buffer, the water logistics chain exhibits high resilience. Even during a full month of transport disruption, the survival of the colony remains uncompromised, allowing for logistical maintenance and error recovery.

4 Strengths and Weaknesses

4.1 Strengths

4.2 Weaknesses and Possible Improvement

5 Conclusion

References

[1] Gunter's Space Page. *Falcon-9*. https://space.skyrocket.de/doc_lau/falcon-9.htm. Accessed: 2026-02-01. Gunter's Space Page, 2026.

[2] Zephyr Penoyre and Emily Sandford. *The Spaceline: a practical space elevator alternative achievable with current technology*. 2019. arXiv: 1908.09339 [astro-ph.IM].

Report on Use of AI

1. OpenAI ChatGPT (Nov 5, 2023 version, ChatGPT-4,)

   Query1: <insert the exact wording you input into the AI tool>

   Output: <insert the complete output from the AI tool>

2. OpenAI Ernie (Nov 5, 2023 version, Ernie 4.0)

   Query1: <insert the exact wording of any subsequent input into the AI tool>

   Output: <insert the complete output from the second query>

3. Github CoPilot (Feb 3, 2024 version)

   Query1: <insert the exact wording you input into the AI tool>

   Output: <insert the complete output from the AI tool>

4. Google Bard (Feb 2, 2024 version)

   Query1: <insert the exact wording of your query>

   Output: <insert the complete output from the AI tool>